Canadian Science Publishing | Transactions of the Canadian Society for Mechanical Engineering

Experimental Investigation of the Internal Tube Flow Effect on the Vibration Response of the Tubes in Shell and Tube Heat Exchanger

Journal:	*Transactions of the Canadian Society for Mechanical Engineering*
Manuscript ID	TCSME-2018-0159.R2
Manuscript Type:	Article
Date Submitted by the Author:	28-Aug-2019
Complete List of Authors:	Ali, Muhammad Nouman; University of Engineering and Technology, Mechanical Engineering; Khushnood, Shahab; University of Engineering and Technology, Mechanical Engineering Nizam, Luqman; University of Engineering and Technology, Mechanical Engineering Bashir, Shahid; University of Engineering and Technology, Mechanical Engineering Hafeez, Akmal; University of Engineering and Technology, Mechanical Engineering
Keywords:	Tube Bundle, Vibration Response, Damping, Cross-Flow, Normal Triangular
Is the invited manuscript for consideration in a Special Issue? :	Not applicable (regular submission)

Experimental Investigation of the Internal Tube Flow Effect on the Vibration Response of the Tubes in Shell and Tube Heat Exchanger

Nouman Ali*, Shahab Khushnood, Luqman Ahmad Nizam, Shahid Bashir, Akmal Hafeez

Department of Mechanical Engineering, University of Engineering and Technology, Taxila, Pakistan.

Corresponding Author E-mail: m.noumanali99@gmail.com

Abstract

In shell and tube heat exchangers, tube bundles often fail due to the flow-induced vibrations. In the current study, vibration response of the tubes, placed in the first and third row of the tube bundle, has been examined having a normal triangular arrangement with pitch-to-diameter (*P/D*) ratio of 1.44. Each tube is tested for three different inside tube flow velocities of 0.85, 0.9 and 1 m/s and five shell side velocities ranging from 0.9 to 1.3 m/s with an increment of 0.1 m/s. This is the first experiment of its kind that offers insight into the tube vibration behavior made of glass material. The experimental analysis shows that tubes with internal flow vibrate with higher amplitudes than tubes without internal flow. Furthermore, the vibration amplitude of the tube tends to rise with increase in internal tube velocity even for the same shell side velocity. For the current range of shell and tube side velocity, with the internal flow from the tube, the hydrodynamic mass of the tube increases significantly with enhanced damping and contributes towards the stability of the tubes in crossflow, the stability threshold is delayed and higher shell side velocities are allowed to enhance the heat transfer rate.

Key words: Cross-flow; Normal triangular; Internal tube flow; Damping

1. Introduction

Heat exchangers are an important and critical part of industries and power plants. It is of much interest to study the instabilities in a heat exchanger to avoid damage and shut down. 'Flow-Induced Vibrations' (FIV) are of key concern in the design of heat exchangers. FIV is characterized as 'fluidelastic instability' (FEI), acoustic resonance, vortex-induced instability (VIV) and turbulence (Weaver & Fitzpatrick, 1988). Vortex induced vibration analysis is carried out for different parameters like 'reduced velocity' and natural frequency for a given mass ratio (Tu et al., 2014). A numerical study was also carried out for cylinders of different diameter and it was found that the cylinder collision depends on the difference of; 'reduced velocity' (Rahmanian, Cheng, Zhao, & Zhou, 2014). Vortex induced vibration effectively reduces for a pipe of small diameter. The Small pipe also leads to a lift force on the oscillating system (Zang & Gao, 2014). Lift coefficient strongly depends on the *P/D* ratio and has an increasing trend with the increase in *P/D* (M. J. Pettigrew & Taylor, 2003). Lift coefficient increases with the increase of cylinder amplitude and lift coefficient will diminish if cylinder amplitude increases one half of the diameter(R. D. Blevins, 1990). The results conclude that; amplitude displacement is directly related to velocity. When the pitch over diameter (P/D) ratio increases around 2 to 4, the amplitude displacement of tubes decreases. It is also investigated that, between staggered and inline arrangements, there is more amplitude displacement of staggered in comparison with inline arrangement for constant tube spacing (Tandel & Patil). The test results also reveal that inclination angle has an inverse relation with crossflow oscillations with peak amplitude for both the inclined bare and inclined helically stacked cylinders. The suppression ratio remained unchanged for inclined as well as vertical cylinders (Zeinoddini, Farhangmehr, Seif, & Zandi, 2015). The natural frequency of the tubes that corresponds to the vibration level in the tube bundle is of prime concern

for the designers. Research regarding flow-induced vibrations has been carried out to relate its field importance and industrial application.

Moreover, the most important excitation phenomena and the leading cause of tube failure in exchangers is fluid-elastic instability. Little tube displacement is induced by the turbulence in the flow so, pattern of flow and forces of fluid changes by this displacement on the tube. More displacement in the tubes is induced by this alteration. The fluid-elastic instability arises if displacement goes on increasing (Price, 1995). Also, the completion of each fluid flow cycle causes the net work done on the moving tubes. Thus, absence of space between the tubes of tube bundle results in "phenomena of jet switch" among strongly packed bundles of tubes. The numerical simulations of elastic-instability of fluid of many cylinders have been performed by researchers under cross-flow conditions (Lin & Yu, 2005). Connors found that elliptical motion model is the most reliable model while analyzing dissimilar models for the prediction of instability (Connors, 1978). He also established that in both, cross-flow and inflow, directions have energy balance which satisfies Eq. (1)

$$\frac{V_{pc}}{f_n D} = K\left(\frac{m\delta}{\rho D^2}\right)^{0.5} \qquad (1)$$

Where K is coefficient of Connors, f_n is tube's natural frequency, m is the ratio of mass, δ is logarithmic decrement, ρ is fluid density, D is the tube outer diameter, and V_{pc} is called the Pitch velocity/Gap velocity and is calculated by the relation existing in Eq. (2) (Connors, 1978).

$$V_{pc} = \frac{VP}{P - D} \qquad (2)$$

Where V is the shell side velocity, and P is tube bundle pitch.

Later on, (R. Blevins, 1979) transformed the Connors model to explain the fluid damping which is flow-dependent, presented in his Eq. (3) (R. Blevins, 1979).

$$\frac{V_{pc}}{f_n D} = K\left[\left(\frac{m\delta}{\rho D^2}\right)2\pi(\zeta_x\zeta_y)^{0.5}\right]^{0.5} \qquad (3)$$

Where ζ_x is the factor of damping, in *x*-direction and ζ_y is the factor of damping in *y*-direction.

It is determined that in the prediction of fluidelastic instability the factor of damping plays a dynamic role in tube bundle (R. Blevins, 1979). When the forces of fluid are just time-dependent function then forced vibration occurs, called as Turbulence Buffeting. The random changes in the flow pattern and the fluid velocity around the tubes are characterized by turbulent flow (R. D. Blevins, 1977). The turbulence in triangular tube array through flow visualization in the water channel and measurements of hot wire in an aerodynamic channel have been studied by researchers (De Paula, Endres, & Möller, 2012). The bank of the tube has a ratio (*P*/*D)* = 1.26 and ranges of Reynolds number from 7.5×10^3 to 4.4×10^4. Visualization reveals the formulation of coalescent jets as flow arises between the gap of tubes. Flow direction changing occurs in a few cases this phenomenon is entitled as metastable. The past third, fourth and fifth-row turbulence features appeared similar to the projected results. In the cross-flow tube vibration of vortex excited is the main mechanism of excitation. A vortices series is produced by the passage of flow over the tube. Alternative forces produced by these series of vortices generate relatively large vibrations in the tube. The frequency of vortex shedding confronted to cross-flow for the single tube is explained by the Eq. (4) (R. D. Blevins, 1977).

$$f_{vs} = \frac{StU}{d_\circ} \qquad (4)$$

Where f_{vs} is the frequency of vortex shedding, *U* is the velocity of the fluid, *St* is the number of Strouhal, and *d*o is cylinder outer diameter.

Over the past few decades, the number of researchers has been investigating the phenomena of vortex shedding. They offered that the tube spacing ratios and vortex shedding frequencies have a relationship between them (Grotz & Arnold, 1956). It is established that in a tube bundle, the

function of tube arrangements for tube banks is Strouhal number with vortex shedding (Lienhard, 1966). Previously internal flow vibrations were studied in shell and tube heat exchangers against the cross-flow for central tube in parallel triangular arrangement with 1.44 pitch to diameter ratio. The shell side velocity and reduced gap velocity was varied from 0.8 m/s to 1.3 m/s and 1.8 to 2.66 respectively. The experiment was carried out without internal flow and with the internal flow. Large amplitude vibration response was observed in subsequent condition. Damping has negligible effects on tube response (Khushnood & Nizam, 2017). Now in this study, tube internal velocity has been varied with varying shell side velocity to analyze the tube vibration response in first and third rows. Both drag and lift direction amplitudes were analyzed. This is the first experiment of its kind that offers insight into tube vibration behavior with varying internal tube velocity in shell and tube heat exchanger made of glass material.

2. Experimental Setup

The experiment was performed on shell and tube type heat exchanger made of glass (borosilicate) which is connected with the test rig as shown in Table 1. Glass Tube Heat Exchanger Specifications

Figure 1.

Shell side of the heat exchanger was connected with Centrifugal Pump rated 10 horsepower and tube side was connected with Centrifugal Pump rated 3 horsepower, drawing water from a common tank of capacity 250 gallons in a closed loop. On shell side five different velocities were achieved from 0.9 to 1.3 m/s with an increment of 0.1m/s for each of the three tube side velocities of 0.85 m/s, 0.9 m/s and 1 m/s, bypass valves were used to control the flow at different velocities

which were measured by Doppler flow meter installed on inlet pipe. Reduced Shell Side velocities ranged from 0.2687 to 0.3881.

Glass tubes in the bundle of heat exchanges were instrumented with strain gauges in the Wheatstone Bridge Configuration, two gauges along the direction of flow to measure vibration response in lift side and two gauges perpendicular to flow direction to measure vibration response in drag side as shown in Figure 2.

Instrumented tubes were placed in 1st and 3rd row of the tube bundle, as indicated by a black circle in Figure 3. Gauges were mounted in the mid-span of instrumented tubes between baffles in the lift and drag direction.

Figure 4 shows the tube properties and schematic layout of supports. Both tubes have the same schematic but differ in position. Fixed gauges on the tube were configured as full Wheatstone bridge and connected with sensing device SG-LINK made by Micro Strain Corporation, USA. Signals from SG-LINK were transferred to Computing device through a wireless base station in the form of graphical time displacement.

Wires from strain gauges were connected to the node of wireless SG-LINK. Signals were interchanged from strain to displacement by this node and sent to WSDA base Station which is directly linked with Computer.

Node commander software was used to operate SG-LINK and signals were collected in the form of live streaming graphs at the sampling rate of 736 samples per second. SIGVIEW software was further used for data extraction from signals and analysis. Signals from the sensor using SIGVIEW software RMS amplitude was calculated at three different points then average value was

considered for lift as well as drag and then resultant RMS Amplitude was calculated from both lift and drag RMS (Root Mean Square) values by Eqs. (5) and (6).

$$Amplitude\ RMS = Amplitude\ Peak/\sqrt{2} \quad (5)$$

$$R = \sqrt{((Lift\ RMS)^2 + (Drag\ RMS)^2}. \quad (6)$$

3. Results and discussions

3.1. Vibration amplitude response

According to previous literature, vibration amplitude response is the most important factor to be analyzed during crossflow for the analysis of flow-induced vibration. (Connors, 1978). In this experimental study, there were two targeted tubes located at a different position but at same velocity scheme. Firstly, tube vibrations in lift and drag were analyzed without internal tube flow (only shell-side flow) and then with both shell and tube side flows with varying velocities. Comparison of the amplitude response of both tubes is shown in Figure 5 & Figure 6.

Figure 5 shows that the vibration response of target tube 1 having no inside flow. There is a negligible rise initially in RMS amplitude of lift and drag up to pitch velocity of 3.25m/s and then almost linear and approximately the same RMS amplitude of lift and drag from 3.25 m/s to 4 m/s. Then there is a rise in lift RMS amplitude at a velocity of ~ 4 m/s, which keeps on increasing. Overall an increasing trend can be noted with the increase of pitch velocity.

Vibration response of target tube 3 having no inside flow is shown in Figure 6. Drag and lift RMS amplitude increases with increase in pitch velocity. The increase in drag is more than lift. There is no significant rise in drag RMS amplitude up to the velocity of ~3.3 m/s. The increasing trend of lift RMS amplitude is quite linear.

The vibration response of target tube 1 when internal tube flow velocity varies is presented in Figure 7. The variations of velocity were 0.85 m/s, 0.9m/s and 1 m/s. Increase in tube flow velocity results in an increase in vibration of the tube in both lift and drag.

Similarly, Figure 8 presents the vibration response of target tube 3 with internal tube flow. The variations of velocity were 0.85 m/s, 0.9m/s and 1 m/s. At 0.85 m/s and 0.9 m/s the lift and drag both have the same and mild increase in RMS amplitude. At velocity rate of 1 m/s lift had a visible increase in RMS amplitude.

The amplitude response of target tube 1 is presented in Figure 9 against different velocities in the tube side as well as shell side. With an increase in the tube side velocity from 0.85m/s to 1 m/s the amplitude response increased gradually. The rate of this increase is relative to shell side velocity.

Figure 10 presents the amplitude response of target tube 3 against the different velocities of the shell side as well as the tube side. All shell side velocities show a gradual increase in amplitude response from 0 m/s to ~0.8 m/s of tube side velocity then after this point sudden increase in amplitude till 1 m/s of tube side velocity. Increase in both tube side velocity as well as shell side velocity causes the maximum amplitude response.

3.2. Damping

Damping is known as the intervention of energy dissipation from a vibrating structure. Damping has great effects on vibration amplitude and amplitude decreases because of energy extraction by dampers provided in the body. In heat exchangers significantly small value of damping is found (R. D. Blevins, 1977). In FIV, an increase in the amplitude of vibration can cause tube bundle or structural damage if energy provided by flow is not dissipated. (Khushnood, 2005). To find log

decrement and Damping Factor the mathematical relationships are used presented in Eqs. (7) and (8) (R. Blevins, 2001).

$$\zeta = {f_2 - f_1}/{2f_n} \quad (7)$$

$$\delta = {2\pi\zeta}/{\sqrt{1-\zeta^2}} \quad (8)$$

Where zeta ζ is a damping factor, δ is the log decrement, and f_1, f_2, and f_n are the frequencies taken from the bode plot.

The log decrement specifies how fast decay of amplitude is in the vibrating tubes. The quicker, the vibration amplitude decay, the greater will be the structure damping (R. D. Blevins, 1977).

Figure 11 shows the plot of the damping factor of the monitored tube in the lift and drag directions for different internal tube flow conditions as a free stream velocity function. Although the plot does not show a definite trend of the damping with an increase in the free stream velocity but seems to be fluctuating around a constant trend. The analysis shows that there is a shift in the mean value of damping as the tube side velocity increases. For tube 1, the damping values are less and fluctuates around mean of 0.01. However, for the tube 3, the mean damping value jumps to around 0.02 mainly due to the fact that as shell-side flow penetrates deep into the bundle, it accelerates and offers more damping. Furthermore, as the tube 3 passes from both baffle holes as compared to the tube 1 (which passes from the one baffle hole), the clearance between the tube and baffle hole offers squeeze film damping results in the higher damping as compared to the tube 1. Uncertainty in damping values ranges from 0.2% to 0.8%.

3.3. Stability Analysis

Stability map is one of the most important criteria to understand instability in a single cylinder as well as in a group of cylinders (tube bundle). It is mathematically formulated in terms of two non-

dimensional parameters i.e. 'Mass Damping Parameter' (MDP) and 'reduced velocity', and given by Eq. (1).

Roberts was considered to be the first researcher to study the fluidelastic instability in crossflow. He performed experiments on the row of cylinders in wind tunnel and calculated the values for the constant based on his experimental data i.e. K= 9.8 and b = 0.5. Connors carefully studied the 'fluidelastic instability' in heat exchanger tube bundle and considered that the value of K should be 9.9, which is also in agreement with the Roberts finding. Researchers have been focused on understanding the 'fluidelastic instability' effect with different geometric parameters with the main purpose to develop concrete guidelines for designing of the tube bundle in order to avoid the failure of a heat exchanger. Different models have been proposed to predict the stability boundary based on the geometric parameters of a heat exchanger. It was later recommended that K = 3.3 can be used as a design guideline for all tube bundles. In more recent research, a standard value of K = 3.0 was also suggested for the design of all types of tube bundle(M. Pettigrew & Taylor, 1991).

From the stability analysis Figure 12 and Figure 13, it can be seen that the data points lie well below the theoretical stability boundaries for the tubes with different internal tube flow velocities. Similarly, the data points also lie on the left side of the stability map mainly because of two reasons. Firstly, the range of mass-damping parameter of the tubes is lower because water is used as a working fluid and the shell side velocity range is small due to the flow limitation of the pump. With the internal flow, the hydrodynamic mass of the tube increases significantly and contributes towards the stability of the tubes in crossflow. Also, the vibration amplitudes are very low so the main excitation mechanism is 'turbulence excitation' which is considered to be the stable operation region of the tube heat exchangers. This is due to the fact point lies below the stability boundary in the stable region. Furthermore, the stability threshold is delayed and higher shell side velocities

are allowed to enhance the heat transfer through the tube bundle. However, in order to understand the stability behavior of the tubes at higher 'reduced velocity' values, higher flow rates in the shell side are required.

Conclusion

Experiments have been designed to study the effect of internal tube flow velocity variation on the vibration response of the glass tube under the influence of varying shell side velocity. From the current analysis, the following conclusions can be made:

1. The vibration amplitudes of the tube increases gradually with an increase in the shell side velocity but remain under 0.005% of tube diameter which indicates that turbulence buffeting is the major source of excitation in tubes.
2. With the increase in the tube side velocity, the vibration amplitudes of the tube tend to rise gradually. Also, for higher shell side velocity, the tubes vibrate with higher amplitudes.
3. Tube 3 experiences more damping as compared to tube 1 mainly due to the reason that tube 3 passes from both baffle holes as compared to tube 1 which passes from the one baffle hole, the clearance between the tube and baffle hole offers squeeze film damping resulting in the higher damping as compared to tube 1.
4. With the internal flow, the hydrodynamic mass of the tube increases significantly and contributes towards the stability of the tubes in crossflow. Furthermore, the stability threshold is delayed and higher shell side velocities are allowed to enhance the heat transfer through the tube bundle.

Acknowledgements

The authors gratefully acknowledge the financial and technical support of University of Engineering and Technology, Taxila for carrying out the research.

References

Blevins, R. (1979). Fluid damping and the whirling instability of tube arrays. *Flow-Induced Vibrations*, 35-39.

Blevins, R. (2001). *Flow-Induced Vibrations* (Second Edition). Malabar, Florida 32950: Krieger publishing company.

Blevins, R. D. (1977). Flow-induced vibration. *New York, Van Nostrand Reinhold Co., 1977. 377 p.*

Blevins, R. D. (1990). Flow-induced vibration.

Connors, H. (1978). Fluidelastic vibration of heat exchanger tube arrays. *Journal of Mechanical Design, 100*(2), 347-353.

De Paula, A., Endres, L., & Möller, S. (2012). Bistable features of the turbulent flow in tube banks of triangular arrangement. *Nuclear Engineering and Design, 249*, 379-387.

Grotz, B., & Arnold, F. (1956). *Flow-induced vibrations in heat exchangers*: Stanford University, Department of Mechanical Engineering.

Khushnood, S., & Nizam, L. A. (2017). Experimental study on cross-flow induced vibrations in heat exchanger tube bundle. *China Ocean Engineering, 31*(1), 91-97.

Lienhard, J. H. (1966). *Synopsis of lift, drag, and vortex frequency data for rigid circular cylinders* (Vol. 300): Technical Extension Service, Washington State University.

Lin, T.-k., & Yu, M.-h. (2005). An experimental study on the cross-flow vibration of a flexible cylinder in cylinder arrays. *Experimental thermal and fluid science, 29*(4), 523-536.

Pettigrew, M., & Taylor, C. (1991). Fluidelastic instability of heat exchanger tube bundles: review and design recommendations. *Journal of pressure vessel technology, 113*(2), 242-256.

Pettigrew, M. J., & Taylor, C. E. (2003). Vibration analysis of shell-and-tube heat exchangers: an overview—Part 2: vibration response, fretting-wear, guidelines. *Journal of Fluids and Structures, 18*(5), 485-500.

Price, S. (1995). A review of theoretical models for fluidelastic instability of cylinder arrays in cross-flow. *Journal of Fluids and Structures, 9*(5), 463-518.

Rahmanian, M., Cheng, L., Zhao, M., & Zhou, T. (2014). Vortex induced vibration and vortex shedding characteristics of two side-by-side circular cylinders of different diameters in close proximity in steady flow. *Journal of Fluids and Structures, 48*, 260-279.

Tandel, V. D., & Patil, R. V. Analysis of cross-flow induced vibration in an inline and staggered configuration.

Tu, J., Zhou, D., Bao, Y., Fang, C., Zhang, K., Li, C., & Han, Z. (2014). Flow-induced vibration on a circular cylinder in planar shear flow. *Computers & Fluids, 105*, 138-154.

Weaver, D. t., & Fitzpatrick, J. (1988). A review of cross-flow induced vibrations in heat exchanger tube arrays†† The original version of this paper was prepared for presentation at the International Conference on Flow Induced Vibrations, Bowness-on-Windermere, 12–14 May 1987; proceedings published by BHRA The Fluid Engineering Centre, Cranfield, England (ed. R. King). *Journal of Fluids and Structures, 2*(1), 73-93.

Zang, Z.-P., & Gao, F.-P. (2014). Steady current induced vibration of near-bed piggyback pipelines: Configuration effects on VIV suppression. *Applied Ocean Research, 46*, 62-69.

Zeinoddini, M., Farhangmehr, A., Seif, M., & Zandi, A. (2015). Cross-flow vortex induced vibrations of inclined helically straked circular cylinders: an experimental study. *Journal of Fluids and Structures, 59*, 178-201.

Table 1. Glass Tube Heat Exchanger Specifications

Tube/Shell material	Glass
No. of tubes	19
Tubes arrangement	Normal Triangular
Tube mass per unit length	0.194 kg/m
Tube outer/inner diameter	15.7 mm/11.7 mm
No. of baffles	2
Clearance of baffle hole	0.4 mm
Clearance of shell baffle	2 mm
Fluid of tube side /Temp.	Water/22°C
Fluid of shell side /Temp.	Water/22°C
No. of spans	3 (Equal spans)
Strain Gauges Location	Mid-span
Length of target span	130 mm
Pitch of the tubes	22.7 mm
Pitch to diameter ratio	1.44
Elasticity modulus (glass tube)	60 GPa
Glass tube density	2500 kg/m^3

The list of tables & figure captions

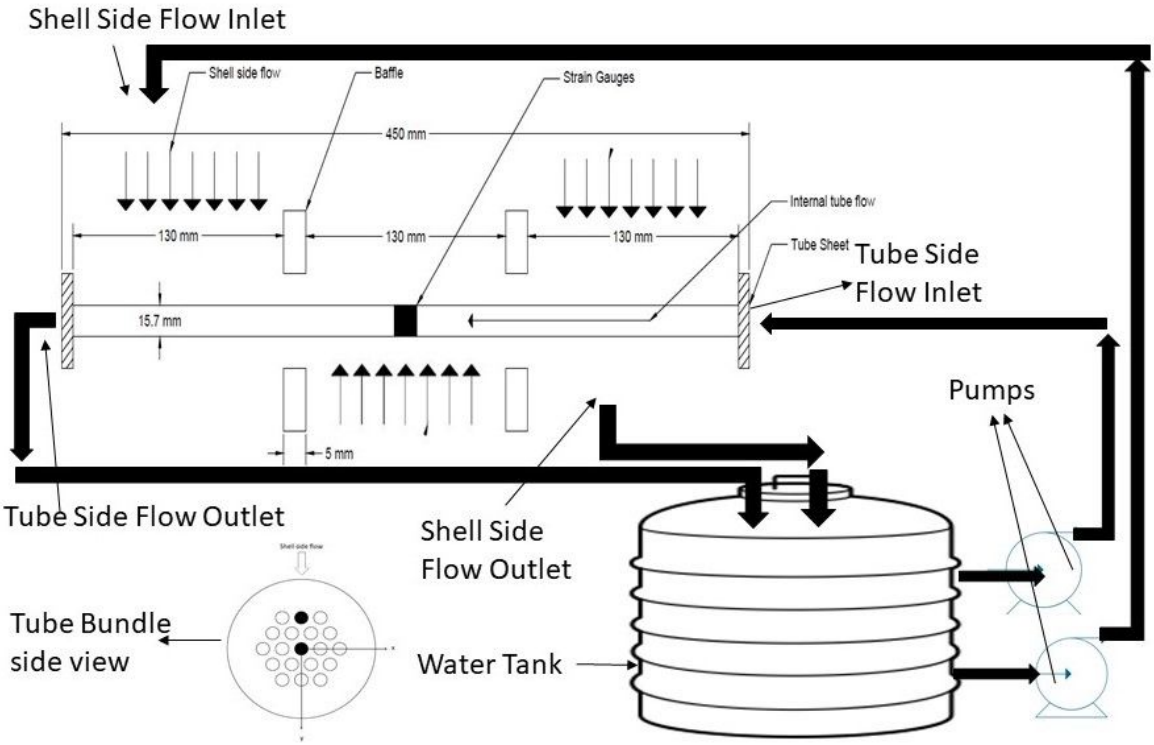

Heat Exchanger setup layout

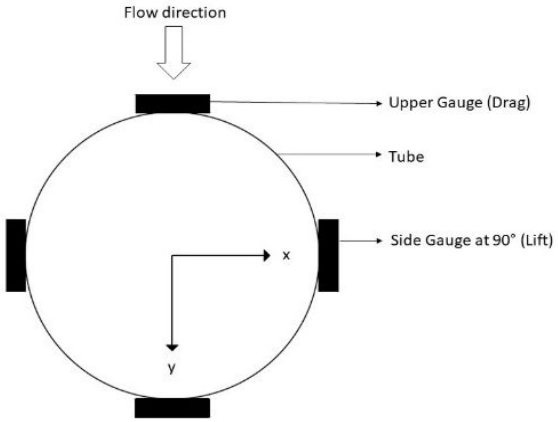

Strain gauges administered on tube in lift & drag direction

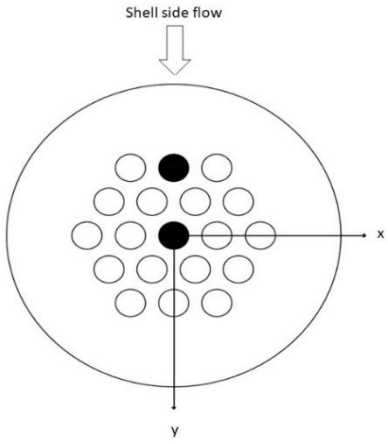

Position of instrumented tubes in tube bundle

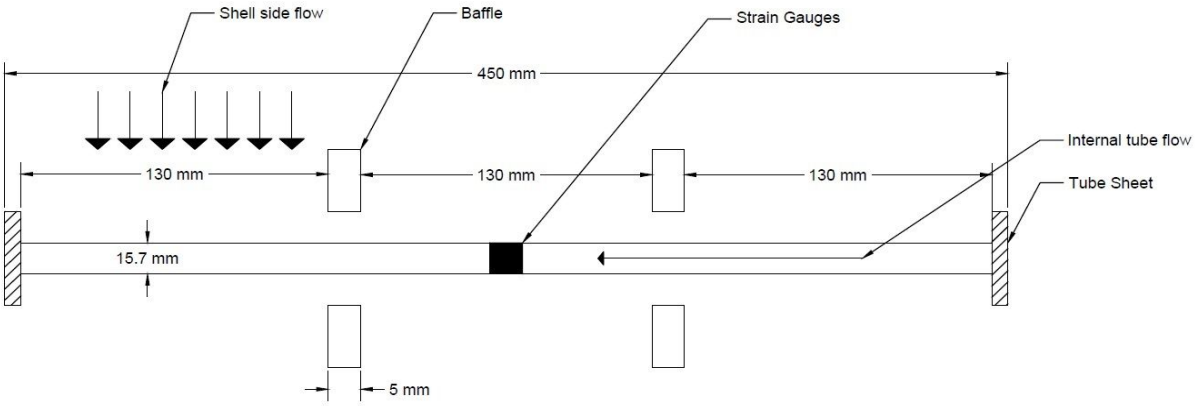

Tube position and supports

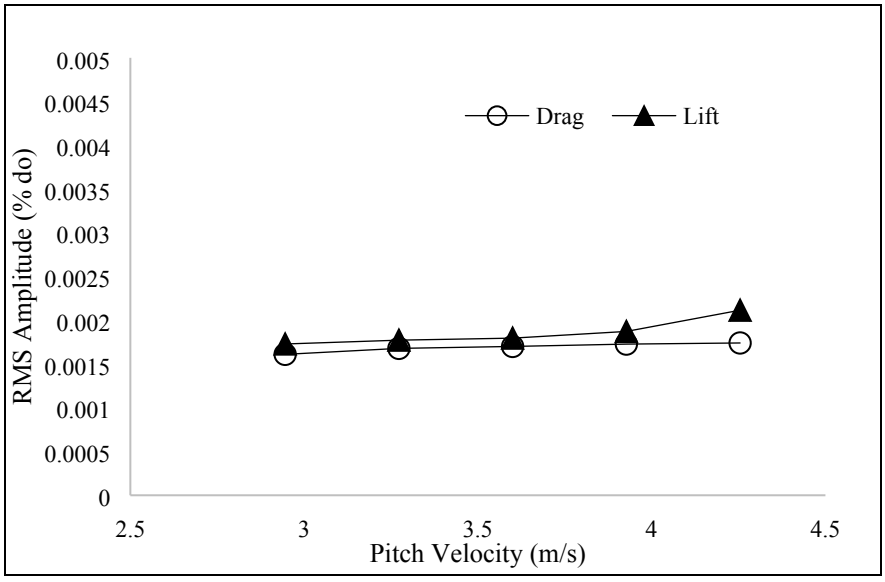

Vibration response of target tube 1 without tube side flow

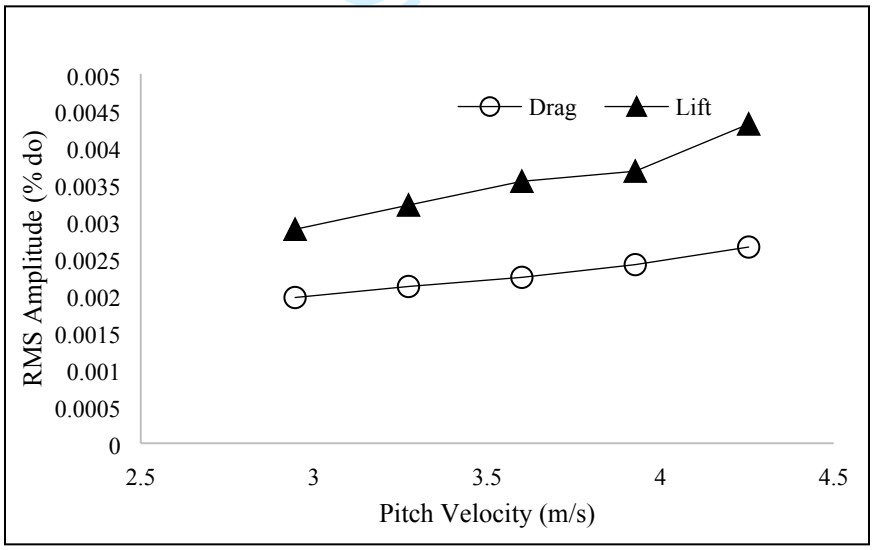

Vibration response of target tube 3 without tube side flow

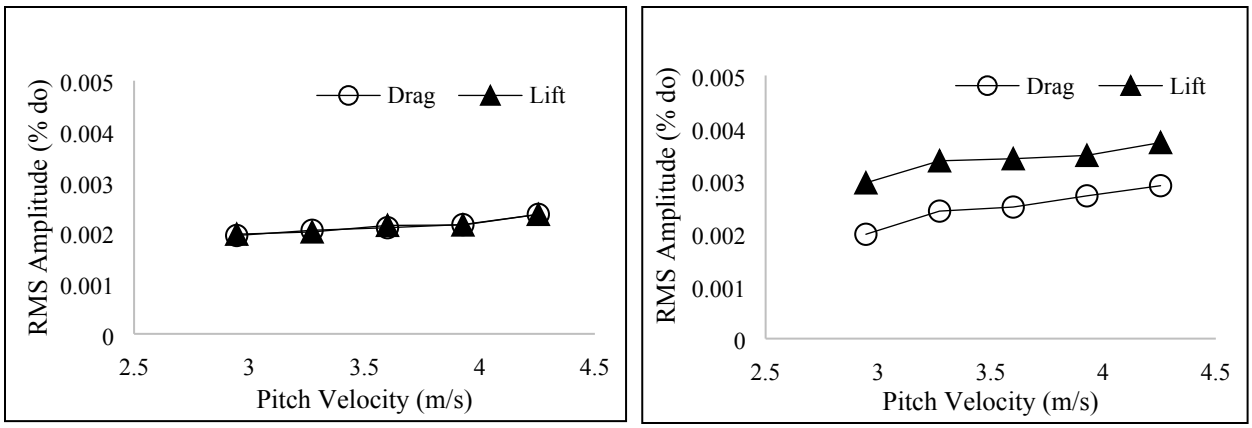

(a) (b)

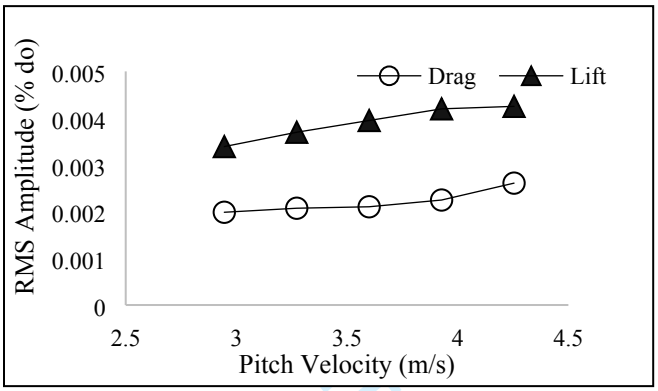

(c)

Vibration response of the target tube 1 with tube flow velocity of (a) 0.85 m/s (b) 0.9 m/s (c) 1 m/s

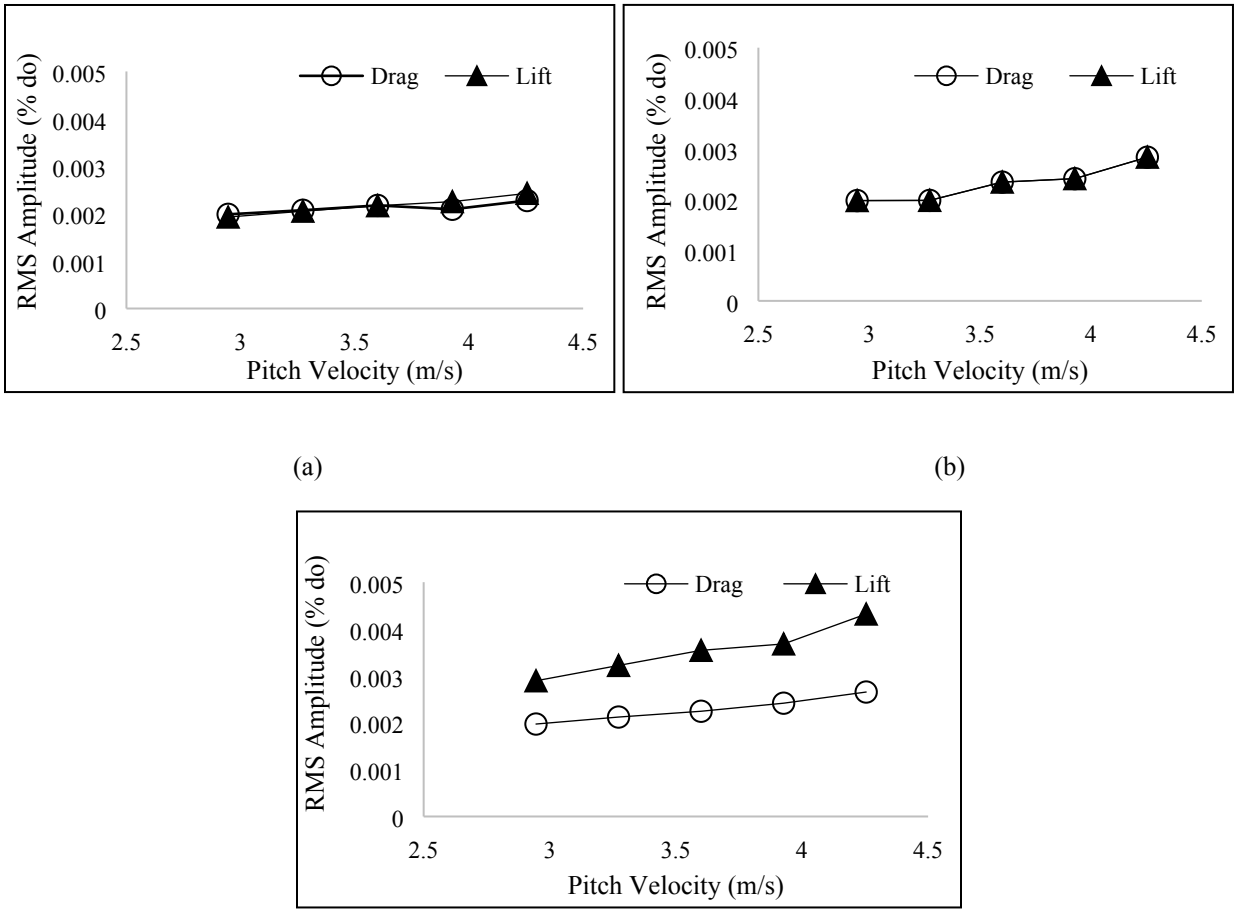

Vibration response of the target tube 3 with tube flow velocity of (a) 0.85 m/s (b) 0.9 m/s (c) 1 m/s

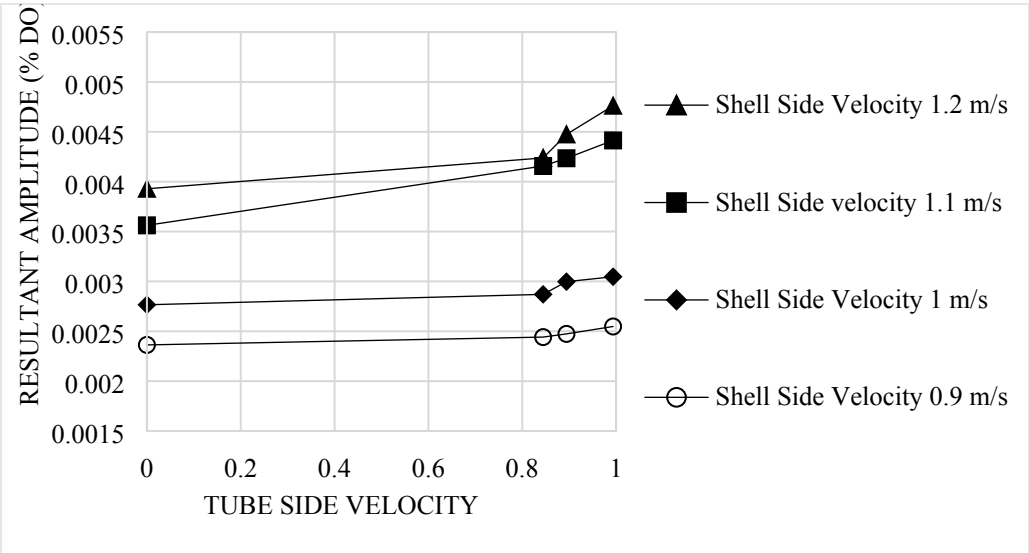

Vibration response of the target tube 1 Shell side velocity

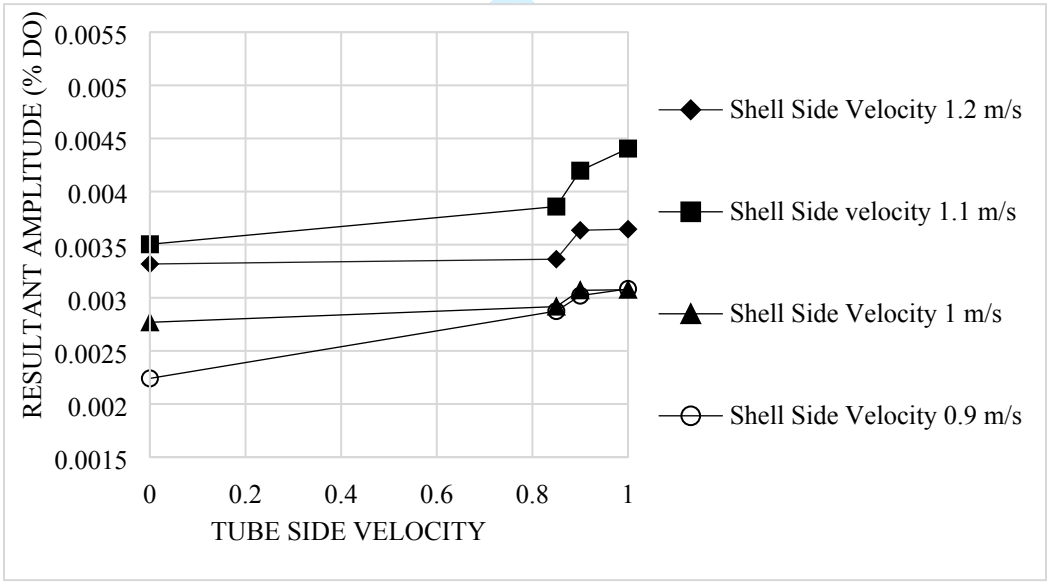

Vibration response of the target tube 3 Shell side velocity

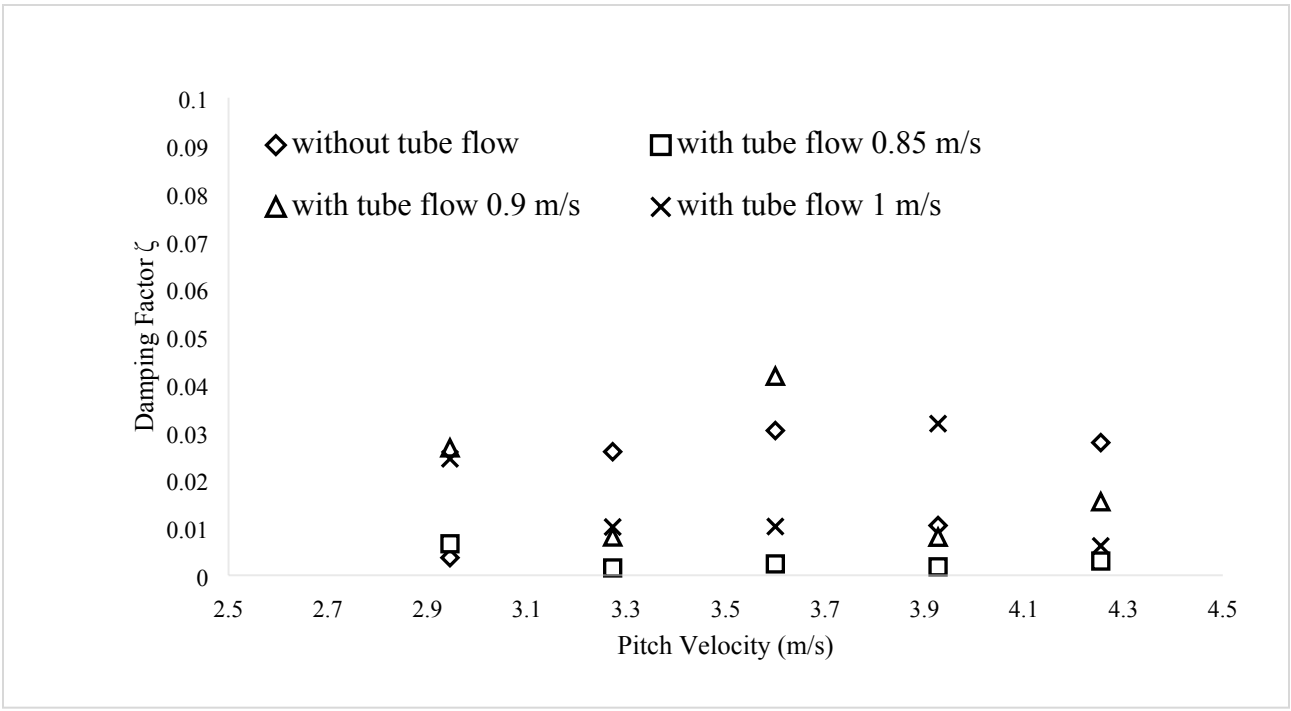

(a)

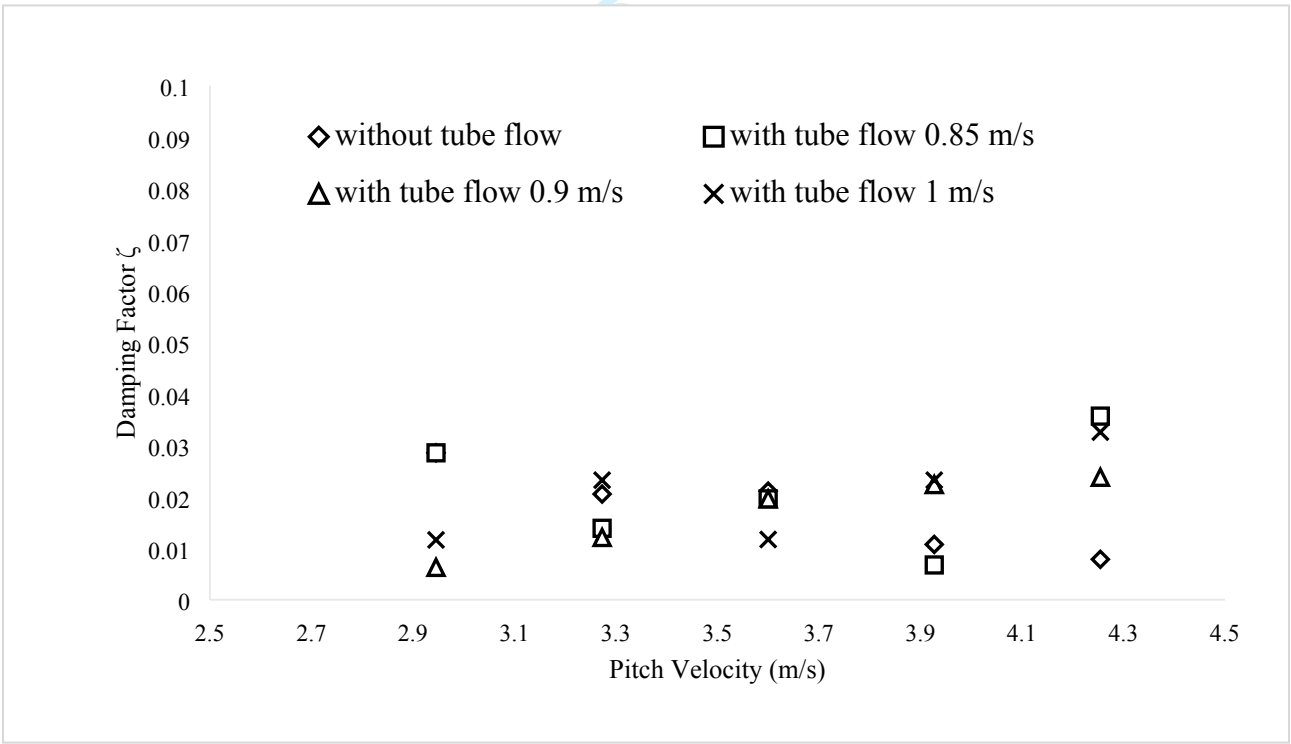

(b)

Damping Factor (a) Tube 1 (b) Tube 3

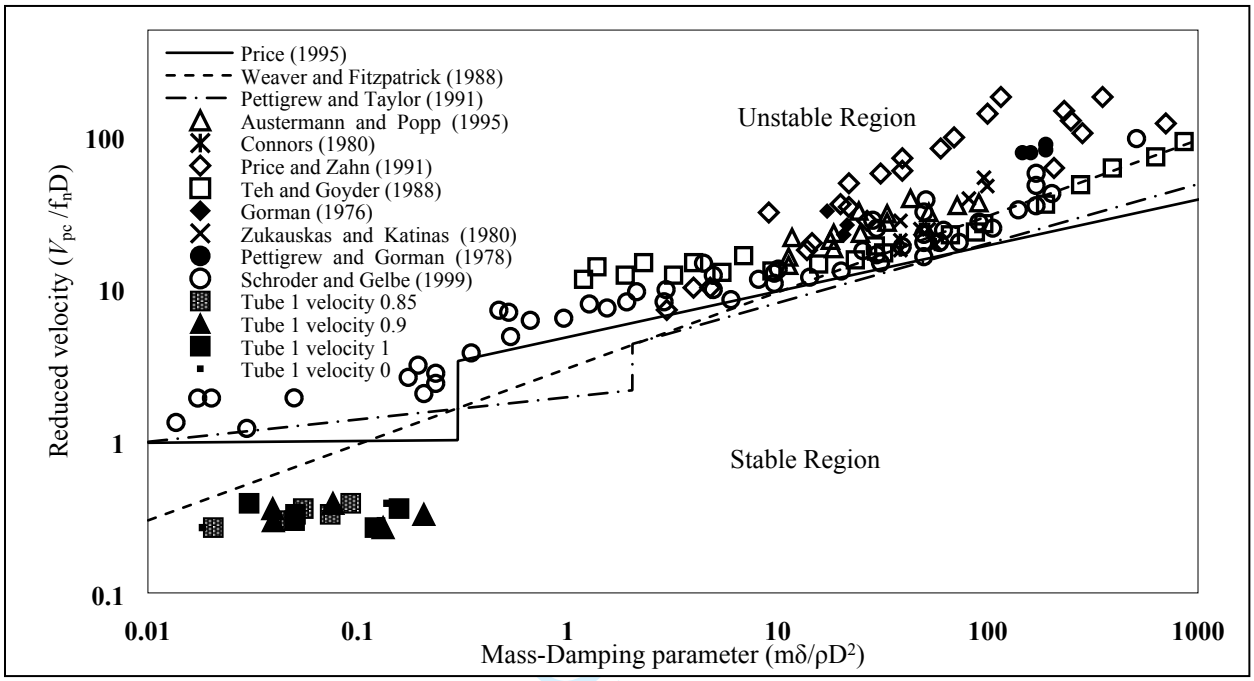

Stability maps for tube 1 P/D ratio 1.44

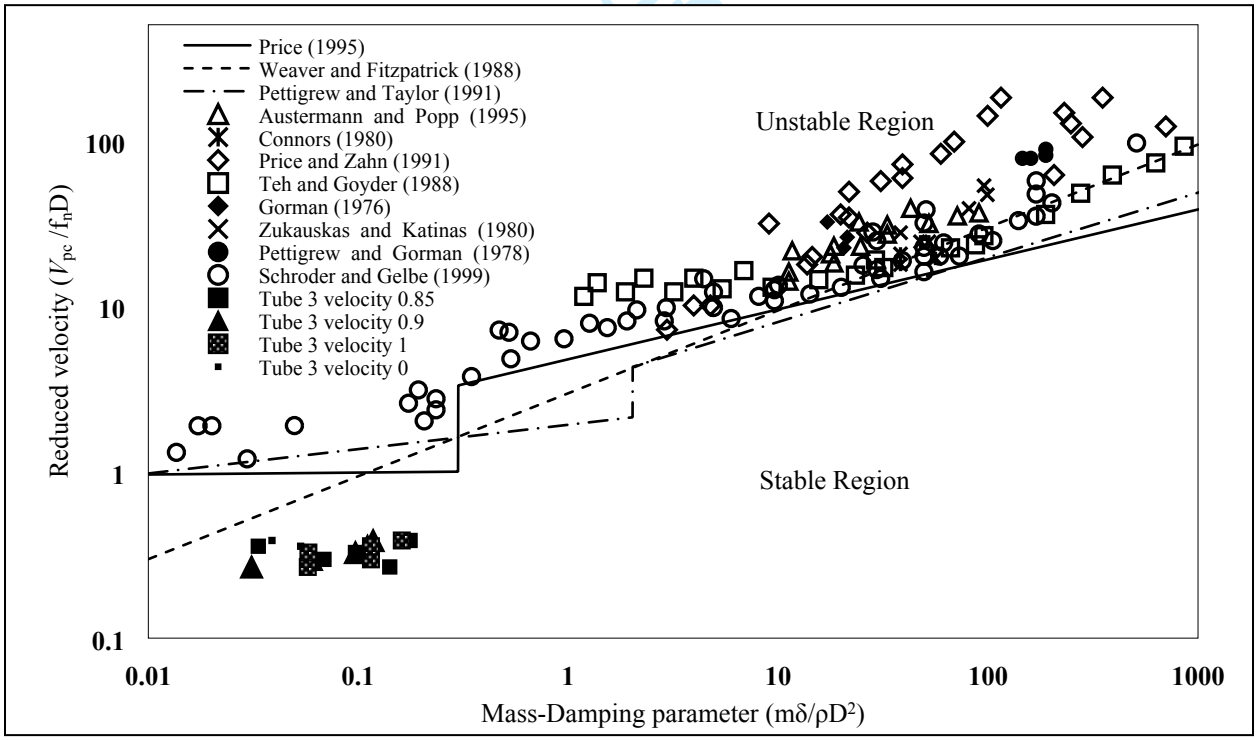

Stability maps for tube 3 P/D ratio 1.44